Supplementary information

Probing conformational variations at the ATPase site of the RNA helicase DbpA by high-field ENDOR spectroscopy

Ilia Kaminker[+], Anastasiya Sushenko[+], Alexey Potapov[+], Shirley Daube[^], Barak Akabayov[%], Irit Sagi[%], and Daniella Goldfarb[+], Departments of Chemical Physics[+], Chemical Infrastructure[^] and Structural Biology[%], Weizmann Institute of Science, Rehovot 76100, Israel.

Table S1. Summary of the observed Mg^{2+} coordination in DbpA-related crystal structures.

PDB Structure	Family	Protein Complex	^{31}P ligands	Number of H_2O ligands	A.A.[b] ligands (shortest Mg^{2+}-^{13}C distance)[a]	Carbon atoms with Mg^{2+}-^{13}C <4.2 Å	Ref
2DB3	DEAD	Vasa AMPPnP (PolyU)RNA	γ ^{31}P β ^{31}P	4	None	γ ^{13}C Asp399 α ^{13}C Gly 552	1
2HYI	DEAD	EJC DDX48/eIF4AIII AMPPnP (PolyU)RNA	γ ^{31}P β ^{31}P	3	Thr 89 (3.86Å)	α ^{13}C Gly 340 γ ^{13}C Thr 89 γ ^{13}C Asp187	2
2J0S	DEAD	EJC DDX48/eIF4AIII AMPPnP (PolyU)RNA	γ ^{31}P β ^{31}P	3	Thr 89 (3.2 Å)	α ^{13}C Gly 340 γ ^{13}C Thr 89 α ^{13}C Thr 89	3
1XTJ	DEAD	Uap56 ADP	β ^{31}P (3.46Å)	Not modeled	None	γ ^{13}C Asp196 δ ^{13}C Glu186	4
3FHT	DEAD	Dbp5 AMPPnP (PolyU)RNA	γ ^{31}P β ^{31}P	4	None	α ^{13}C Gly 396 γ ^{13}C Asp242	5
3I5Y	DEAD	Mss116p AMPPnP (PolyU)RNA	γ ^{31}P β ^{31}P	4	None	ε ^{13}C Lys 158	6
2XAU	DEAH	PRP43p	β ^{31}P	4	Thr 129	α ^{13}C	7

		ADP	(3.30Å)		(3.1 Å)	Thr 129 β ^{13}C Thr 129 (CH3) Thr 129	
3LLM	DEAD(Mutation) Mn^{2+} cofactor	DHX9 ADP	β ^{31}P (3.18Å)	3	Thr418 Glu512 (3.05 Å)	β ^{13}C Thr 418 δ ^{13}C Glu186 (3.05A)	[8]
3XK2	DEAH	PRP43p ADP	β ^{31}P (3.38Å)	4	Thr 123 (3.16 Å)	α ^{13}C Thr 123 β ^{13}C Thr 123 (CH3) Thr 123	[9]
3G0H	DEAD	Ddx19 AMPPnP (PolyU)RNA	γ ^{31}P β ^{31}P	Not modeled	None	α ^{13}C Gly 396	[10]
2PL3	DEAD	DDX10 ADP	β ^{31}P (3.38Å)	4	Glu223 (3.11 Å)	δ ^{13}C Glu186 (3.11A) γ ^{13}C Glu186	

[a] Coordinated to Mg^{2+} via a directly bound oxygen. [b] A.A. – amino acids

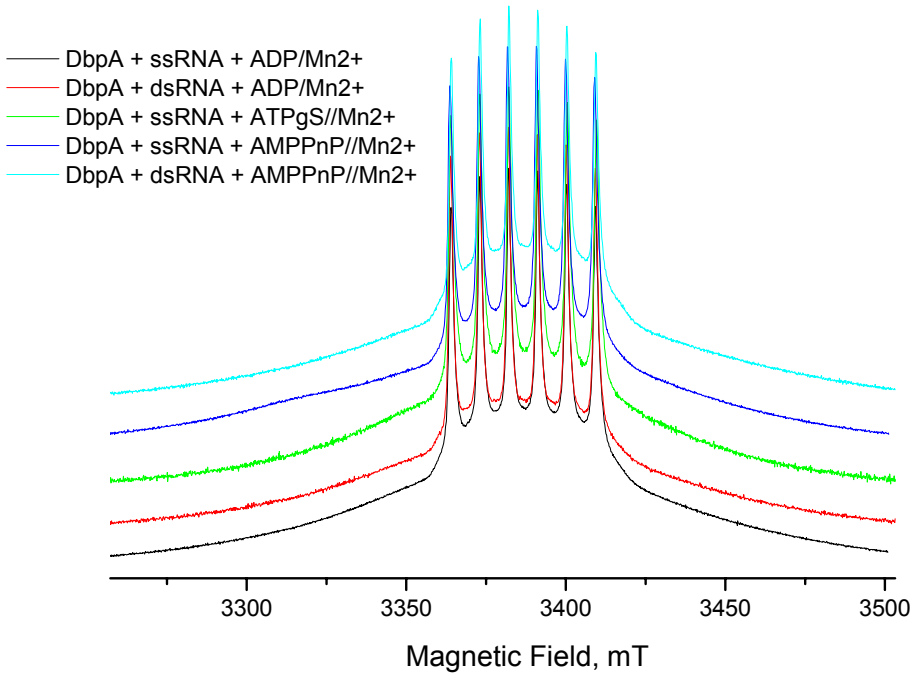

Figure S1. Echo-Detected EPR spectra of several representative DbpA/Mn^{2+}/Nucleotide/RNA complexes as indicated in the Figure.

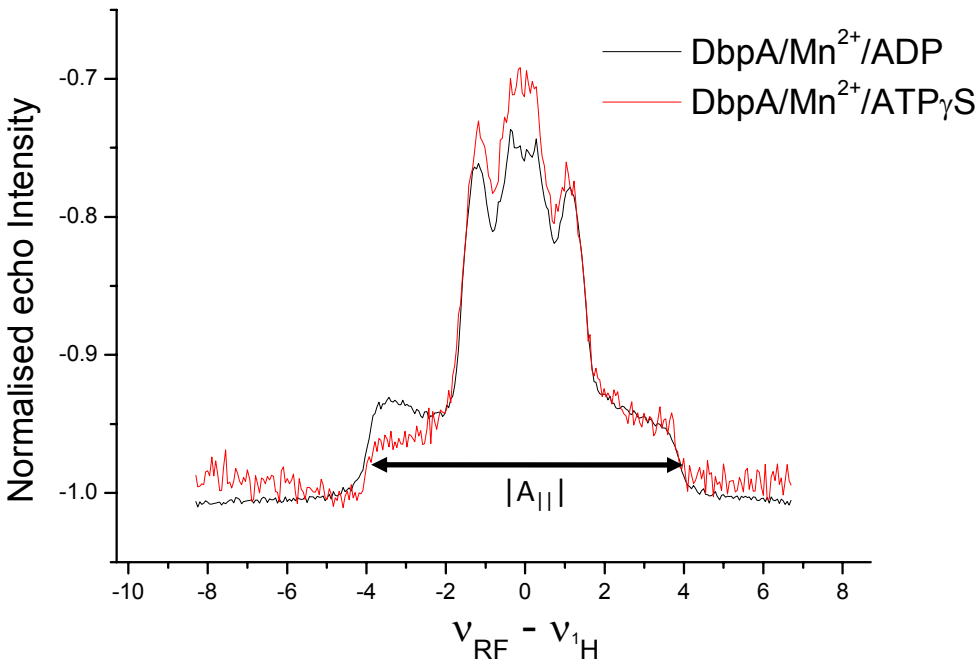

Figure S2. Sample ^{1}H Davies ENDOR spectra. Experimental parameters: $\pi/2$ / π MW pulses 100ns / 200ns respectively, length of the RF pulses was 25μs and τ was set to 400ns. The largest observed hyperfine of ~8MHz is characteristic of $|A_{||}|$ of a directly coordinated water ligand.[11]

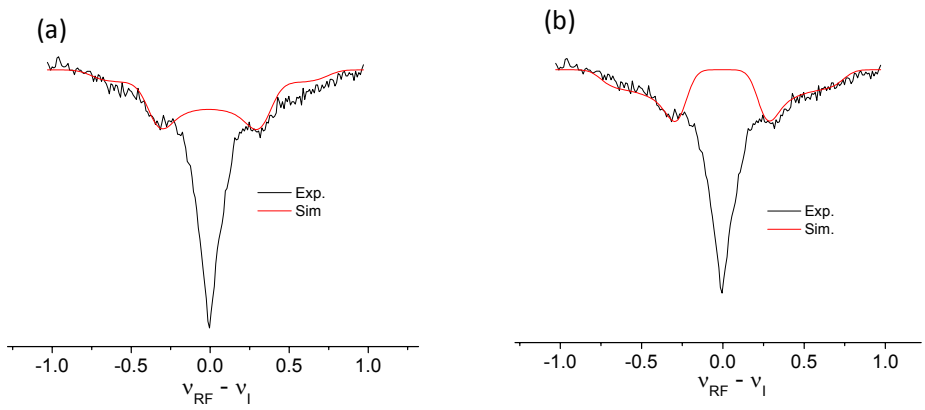

Figure S3. Simulations (red) of the ^{13}C ENDOR spectra (black) for the DbpA/Mn^{2+}/AMPPnP/ssRNA complex. Hyperfine parameters used in the simulations were: (a) $A_{\|}$ = 1.4MHz, $A_{\perp}$ = -0.7MHz. (b) $A_{\|}$ = 1.5MHz, $A_{\perp}$ = 0.5MHz;

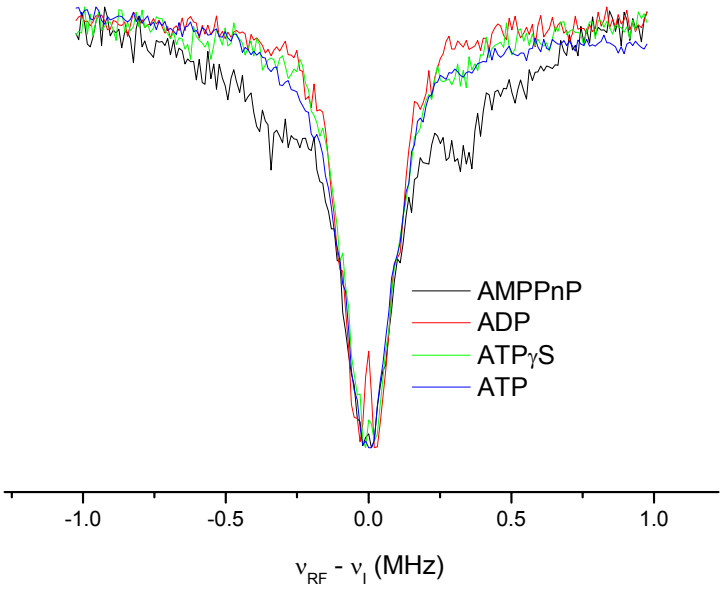

Figure S4. Comparison of the ^{13}C ENDOR spectra of the DbpA/Mn^{2+}/nucleotide complexes without RNA. The type of the bound nucleotide is indicated in the figure legend.

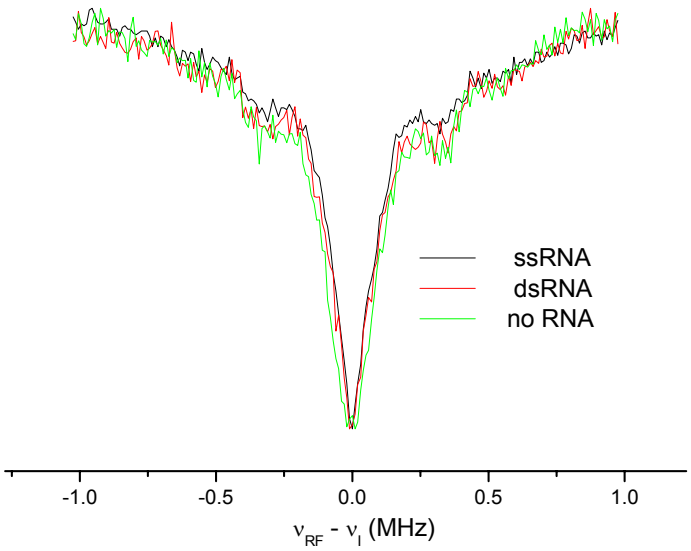

Figure S5. Comparison of the AMPPnP-bound complexes. The type of RNA cofactor is indicated in the Figure legend.

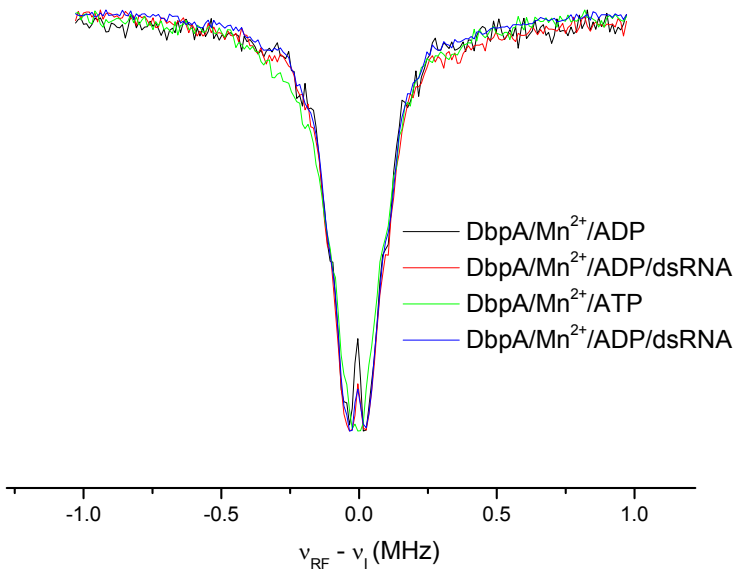

Figure S6. Comparison of the DbpA/Mn^{2+}/ADP(ATP) complexes with and without dsRNA as indicated in the figure.

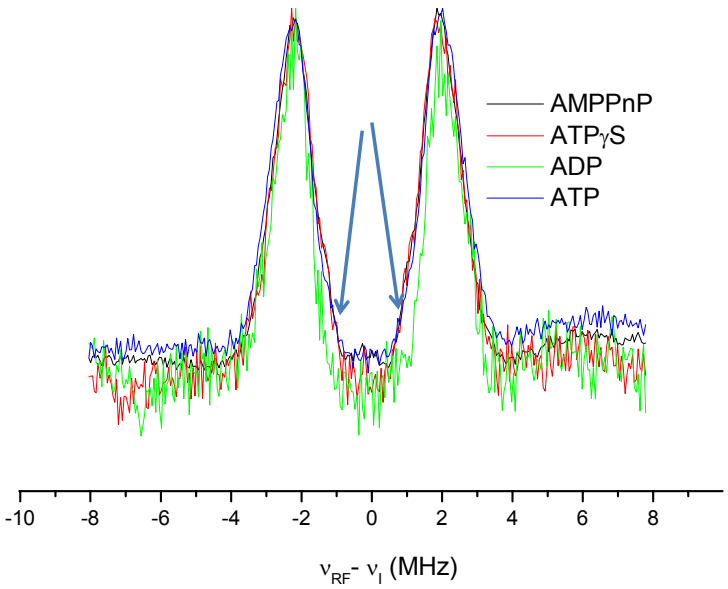

Figure S7. Overlay of the ^{31}P ENDOR spectra of the Mn^{2+}/nucleotide complexes, without DbpA and without RNA. The type of the bound nucleotide is noted in the Figure legend. Arrows indicate the position where the difference between the ADP and ATP-analog bound spectra is most pronounced.

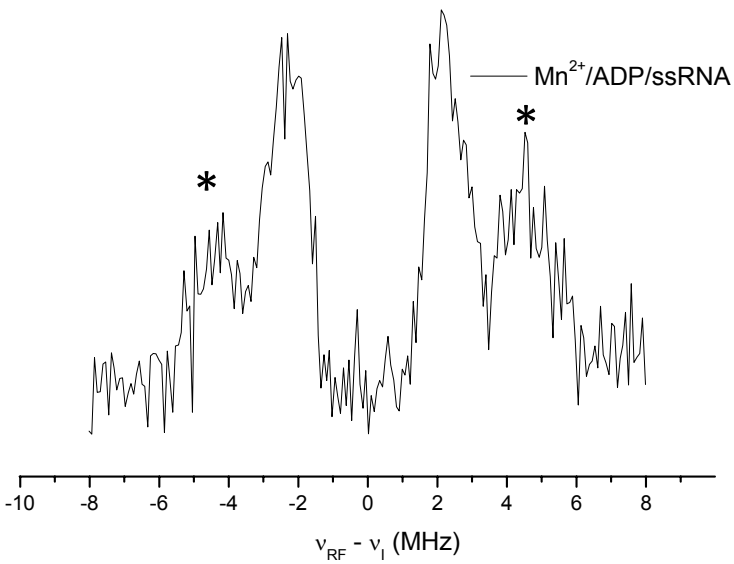

Figure S8. ^{31}P ENDOR spectrum of the ssRNA/ADP/Mn^{2+} complex (no DbpA). * - denotes the ~9MHz coupling of Mn^{2+} bound to the RNA phosphates.

ATPγS hydrolysis measurements: ATPγS and ATP hydrolysis rates were measured under conditions of the concentration range of the EPR samples used in this work but with Mg^{2+} instead of Mn^{2+}. Reaction conditions: [DbpA] = [RNA] = 0.16mM, [ATP] ([ATPγS]) = 0.4mM, [Mg^{2+}] = 0.4mM. The reaction was initialized by adding the Mg^{2+}/ATP (or Mg^{2+}/ATPγS) mixture, supplemented with trace amounts of ATγ^{32}P or ATPγ^{35}S (Perkin Elmer), respectively, to the preincubated RNA/DbpA mixture. The reaction was sampled by extracting 1 μl of the reaction mixture into a 4-μl stop solution (0.2% SDS / 20 mM EDTA final concentrations). 1μl of each time point was then spotted on a polyethyleneimine (PEI) cellulose Thin Layer Chromatography (TLC) plate. ATP and its analog were resolved from their Pi and ^{35}S-Pi hydrolysis products, respectively, by developing the TLC plate in 0.3 M potassium phosphate, pH=7.0. TLC plates were dried and imaged by exposing to a phosphorous screen (FUJI) that was then scanned by a phosphorimager (FLA-5100, FUJI) . Images were quantified using Image Gauge (Fuji) and ATP hydrolysis rates were calculated from the ratio of AT^{32}P or ATPγ^{35}S to ^{32}Pi or ^{35}S-Pi, respectively. Figure S7 shows the results of such a measurement. It confirms that under our experimental conditions ATP and ATPγS are essentially hydrolyzed with a similar rate. Moreover, after 5 minutes, which is a reasonable time between sample preparation and freezing, >90% of the ATPγS already underwent hydrolysis. This independently supports our ENDOR-based observation that ATPγS undergoes rapid hydrolysis under the EPR experimental conditions.

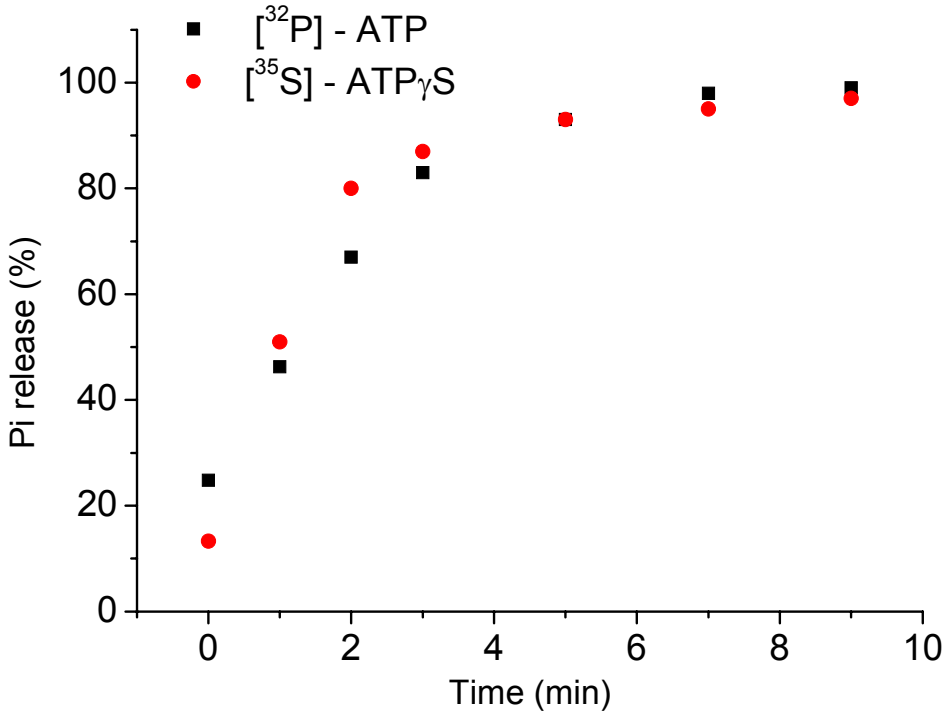

Figure S8. Comparison of the ATPγS and ATP hydrolysis rates measured under conditions similar to the EPR samples used in this work. The measurements were performed using ^{32}P- and ^{35}S-labeled ATP and ATPγS nucleotides, respectively.

References

(1) Sengoku, T. Nureki, O. Nakamura, A. Kobayashi, S.; Yokoyama, S. *Cell* **2006**, *125*, 287-300.
(2) Andersen, C. B. F. Ballut, L. Johansen, J. S. Chamieh, H. Nielsen, K. H. Oliveira, C. L. P. Pedersen, J. S. Seraphin, B. Hir, H. L.; Andersen, G. R. *Science* **2006**, *313*, 1968-1972.
(3) Bono, F. Ebert, J. Lorentzen, E.; Conti, E. *Cell* **2006**, *126*, 713-725.
(4) Shi, H. Cordin, O. Minder, C. M. Linder, P.; Xu, R.-M. *Proc. Natl. Acad. Sci. U. S. A.* **2004**, *101*, 17628 -17633.
(5) von Moeller, H. Basquin, C.; Conti, E. *Nat. Struct. Mol. Biol.* **2009**, *16*, 247-254.
(6) Del Campo, M.; Lambowitz, A. M. *Mol. Cell* **2009**, *35*, 598-609.
(7) Walbott, H. Mouffok, S. Capeyrou, R. Lebaron, S. Humbert, O. van Tilbeurgh, H. Henry, Y.; Leulliot, N. *EMBO J.* **2010**, *29*, 2194-2204.
(8) Schütz, P. Wahlberg, E. Karlberg, T. Hammarström, M. Collins, R. Flores, A.; Schüler, H. *J. Mol. Biol.* **2010**, *400*, 768-782.
(9) He, Y. Andersen, G. R.; Nielsen, K. H. *EMBO. Rep.* **2010**, *11*, 180-186.
(10) Collins, R. Karlberg, T. Lehtiö, L. Schütz, P. van den Berg, S. Dahlgren, L.-G. Hammarström, M. Weigelt, J.; Schüler, H. *J. Biol. Chem.* **2009**, *284*, 10296 -10300.
(11) Manikandan, P. Carmieli, R. Shane, T. Kalb (Gilboa), J.; Goldfarb, D. *J. Am. Chem. Soc.* **2000**, *122*, 3488-3494.